



Article

Impact of Temperature and Nanoparticle Concentration on Turbulent Forced Convective Heat Transfer of Nanofluids

Janusz T. Cieśliński ^{1,*} , Dawid Lubocki ¹ and Sławomir Smolen ² 

¹ Faculty of Mechanical Engineering and Ship Technology, Institute of Energy, Gdańsk University of Technology, Narutowicza 11/12, 80233 Gdańsk, Poland

² Faculty of Nature and Engineering, J.R. Mayer–Institute for Energy Engineering, City University of Applied Sciences Bremen, Neustadtswall 30, 28199 Bremen, Germany

* Correspondence: jcieslin@pg.edu.pl

Abstract: Theoretical analysis of the influence of nanoparticles and temperature on the average Nusselt (Nu) number and the average heat transfer coefficient (HTC) during the turbulent flow of nanofluid in a horizontal, round tube was carried out. The Nu number is a function of the Reynolds (Re) number and the Prandtl (Pr) number, which in turn are functions of the thermophysical properties of the liquid and the flow conditions. On the other hand, the thermophysical properties of nanofluids are primarily a function of nanoparticle concentration (NPC) and temperature. Hence, the correct determination of the value of the Nu number, and then the HTC, which is needed for engineering calculations, depends on the accuracy of determining the thermophysical properties of nanofluids. In most cases, the thermophysical properties of the nanofluids are calculated as functions of the corresponding thermophysical properties of the base liquid. Therefore, the accuracy of the calculations of the thermophysical properties of nanofluids is equally determined by the reliable correlations for the base liquids. Therefore, new correlations for the calculation of the thermophysical properties of water have been developed. The results of calculations of the thermophysical properties of the base liquid (water) and the water-Al₂O₃ nanofluids by use of carefully selected correlations is presented. It was established that even for small concentrations of nanoparticles, a significant intensification of heat transfer using nanofluids as compared to the base liquid is obtained for the tested temperature range.

Keywords: nanofluids; thermophysical properties; forced convective heat transfer; horizontal tube



Citation: Cieśliński, J.T.; Lubocki, D.; Smolen, S. Impact of Temperature and Nanoparticle Concentration on Turbulent Forced Convective Heat Transfer of Nanofluids. *Energies* **2022**, *15*, 7742. <https://doi.org/10.3390/en15207742>

Academic Editor: Dmitry Eskin

Received: 19 September 2022

Accepted: 17 October 2022

Published: 19 October 2022

Publisher's Note: MDPI stays neutral with regard to jurisdictional claims in published maps and institutional affiliations.



Copyright: © 2022 by the authors. Licensee MDPI, Basel, Switzerland. This article is an open access article distributed under the terms and conditions of the Creative Commons Attribution (CC BY) license (<https://creativecommons.org/licenses/by/4.0/>).

1. Introduction

Constant technological progress means that the heat fluxes that occur in devices are increasing. This presents a real challenge for heat transfer engineers and researchers. Two directions of intensification of heat transfer are being developed. The first is related to the modification of the heat exchange surface, e.g., [1–3]. The second is related to the search for new thermal fluids that are characterized by better thermophysical properties, such as thermal conductivity or contact angle. Among the new thermal fluids, the greatest hope is raised by a mixture of a base liquid and nanoparticles with a size below 100 nm, referred to as a nanofluid [4]. The use of nanofluids in a great number of areas is considered, such as single-phase systems, e.g., [5,6], two-phase systems, e.g., [7,8], magnetic nanofluids, e.g., [9,10], non-Newtonian nanofluids, e.g., [11,12], viscoelastic nanofluids, e.g., [13,14], chemical reaction systems, e.g., [15,16], bio-nanofluids, e.g., [17,18], nanofuels, e.g., [19,20], and others [21].

The single-phase convective heat transfer of nanofluids is of particular interest due to potential applications in many cooling/heating systems, e.g., heat exchangers, electronics, nuclear reactors, car radiators, solar devices, e.g., [22–25], medical applications, e.g., [26,27], thermal energy storage, e.g., [28,29], or even rocketry applications [30]. Although different aspects, e.g., flow regimes—laminar or turbulent, boundary conditions, nanoparticle type

and concentration, of single-phase forced convection of nanofluids in tubes were studied both experimentally [31–34] and numerically [35–42] there is still controversy about the influence of nanoparticles on heat transfer efficiency and flow resistance. Experimental works show that the addition of nanoparticles can both intensify and deteriorate heat transfer. In turn, numerical works most often show the intensification of heat transfer as a result of adding nanoparticles. A similar controversy concerns flow resistance. Intensive work is still underway to determine the thermophysical properties of nanofluids and their stability [43,44].

The nanofluid, which is inherently a two-phase mixture of liquid and solid particles, can be modeled as a single-phase continuum (single phase fluid) with the thermophysical properties which take into account the effect of the presence of nanoparticles. The results of numerical simulations obtained with the single-phase approach and the two-phase model [45,46], did not differ significantly. The condition for the accuracy of the single-phase approach is the correct selection of the correlation on the thermophysical properties of nanofluids.

In the present study, a theoretical analysis of the influence of temperature and NPC during forced convection of nanofluids inside a horizontal circular tube is presented. It was assumed that the analyzed nanofluid can be treated as a homogeneous, single-phase liquid. The Nu number and average HTC were parameters of the intensity of the convective heat transfer. For forced convection, the Nu number is a function of the Re number and Pr number. The Re number and Pr number are functions of the thermophysical properties of nanofluids. The thermophysical properties of nanofluids varied first of all with temperature and NPC. Therefore, an analysis was conducted to evaluate the effects on the performance of nanofluids due to variations of thermal conductivity, viscosity, density, and specific heat, which are functions of NPC and temperature. Water-based nanofluids with dispersed alumina (Al_2O_3) nanoparticles at mass concentrations of 0.1%, 1%, and 5% within the temperature range 20–70 °C are considered. Water- Al_2O_3 nanofluids were selected because frequent application in both numerical and experimental studies. Moreover, thermophysical properties of water- Al_2O_3 nanofluids are comprehensively and thoroughly investigated [47].

2. Materials and Methods

2.1. Tested Nanofluids

In this study alumina (Al_2O_3) nanoparticles were selected while distilled, deionized water was tested as base fluid. Alumina nanoparticles were tested at the concentration of 0.1%, 1%, and 5% by weight. It was assumed that nanoparticles have a spherical form with mean diameter of $d_p = 47$ nm.

The properties of alumina (Al_2O_3) nanoparticles are shown in Table 1.

Table 1. Properties of Al_2O_3 nanoparticles.

Thermal Conductivity k_p [W/(mK)]	Density ρ_p [kg/m ³]	Specific Heat $c_{p,p}$ [J/(kg K)]
35 *	3600 **	765 **

*—[48], **—[49].

2.2. Correlations for Forced Convection Heat Transfer inside Horizontal Tubes

Recognized correlation equations used for the determination of an average Nu number for forced convection inside horizontal cylinders in base fluids are collected in Table 2. The Nu number for water is a benchmark to the values calculated for the analyzed nanofluids. Hence, the selection of the correct correlation is important when comparing the results for the base fluid and nanofluids.



Table 2. Correlation equations for turbulent flow of base fluid.

Authors	Correlation	Range	Remarks	Equation
Dittus and Boelter [50]	$\overline{Nu} = 0.23Re^{0.8}Pr^n$	$Re > 10^4$ $0.7 < Pr < 100$	$n = 0.4$ —heating $n = 0.3$ —cooling	Equation (1)
Kraußold [51]	$\overline{Nu} = 0.032Re^{0.8}Pr^n \left(\frac{L}{D}\right)^{-0.054}$	$Re > 10^4$	$n = 0.37$ —heating $n = 0.3$ —cooling	Equation (2)
Sieder and Tate [52]	$\overline{Nu} = 0.027Re^{4/5}Pr^{1/3} \left(\frac{\mu_f}{\mu_w}\right)^{0.14}$	$Re > 10^4$ $0.7 < Pr < 16,700$	$T_w = \text{const.}$	Equation (3)
Mikhejev [53]	$\overline{Nu} = 0.021Re^{0.8}Pr_f^{0.43} \left(\frac{Pr_f}{Pr_w}\right)^{0.25} \epsilon_L$	$10^4 < Re < 5 \times 10^6$ $0.6 < Pr < 2500$	$\epsilon_L = f(L/D, Re)$	Equation (4)
Petukhov [54]	$\overline{Nu} = \frac{(f/8)RePr}{1.07+12.7(f/8)^{1/2} \left(Pr^{2/3}-1\right)}$	$10^4 < Re < 5 \times 10^6$ $0.5 < Pr < 2000$	$f = (1.82\ln Re - 1.64)^{-2}$	Equation (5)
Notter and Sleicher [55]	$\overline{Nu} = 4.8 + 0.0156Pe^{0.85}Pr^{0.08}$ $\overline{Nu} = 6.3 + 0.0167Pe^{0.85}Pr^{0.08}$	$10^4 < Re < 10^6$ $0.004 < Pr < 0.1$	$T_w = \text{const.}$ $q_w = \text{const.}$	Equation (6) Equation (7)
Churchill and Ozoe [56]	$\overline{Nu} = \frac{0.3387Pr^{1/3}Re^{1/2}}{\left[1+(0.0468/Pr)^{2/3}\right]^{1/4}}$	$Re > 100$ $10^{-4} < Pr \rightarrow \infty$	$q_w = \text{const.}$	Equation (8)
Hausen [57]	$Nu = 0.0235 \left[1 + \left(\frac{d}{L}\right)^{2/3}\right]$ $\left[Re^{0.8} - 230\right] Pr_f^{0.3} \left(\frac{\mu_f}{\mu_w}\right)^{0.14}$	$2300 < Re < 2 \times 10^6$ $1.5 < Pr < 500$ $d/L < 1$		Equation (9)
Gnieliński [58]	$\overline{Nu} = \frac{(f/8)(Re-1000)Pr}{1+12.7(f/8)^{0.5} \left(Pr^{2/3}-1\right)}$	$3 \times 10^3 < Re < 5 \times 10^6$ $0.5 < Pr < 2000$	$f = (0.79\ln Re - 1.64)^{-2}$	Equation (10)
Kutateladze [59]	$\overline{Nu} = 1.61 \left(Pe \frac{D}{L}\right)^{1/3}$	$Pe > 12$ $d/L < 12$		Equation (11)

Figure 1 shows the dependence of the Nu number on the Re number on the basis of the correlations shown in Table 1. The calculations were performed for the $Pr = 5$. The values of the correction coefficients were assumed to be equal to one. Noteworthy is the fact that the values of the Nu number are significantly higher from the Notter and Sleicher correlation [55] compared to the other correlations. Note, however, that the Notter and Sleicher correlations (Equations (6) and (7)) are suitable for fluids with a very low Pr number. Figure 1 shows that the correlations proposed by Dittus and Boelter, Kraußold, Sieder and Tate, Mikhejev, Hausen, and Gnieliński give similar values of the Nu number, although the difference between the Kraußold correlation and Hausen correlation for $Re = 10^5$ is as much as 45%.

In Table 3 are collected experimental and numerical correlation equations used for determination of an average Nu number for forced convection inside horizontal cylinders in nanofluids.

Figure 2 shows the dependence of the Nu number on the Re number for nanofluids and correlations shown in Table 3. The calculations were performed for the $Pr = 5$, $w = 1$ m/s, $\varphi_v = 1\%$ and $d_p = 40$ nm.

As seen in Figure 2, except Equation (17), the correlations show pretty good consistency. The numerically developed correlation equation proposed by Saha and Paul, Equation (18), was selected for the analysis, as it fits the experimental data for water- Al_2O_3 nanofluids very well and contains parameters that characterize both nanoparticles and molecules of the base fluid.

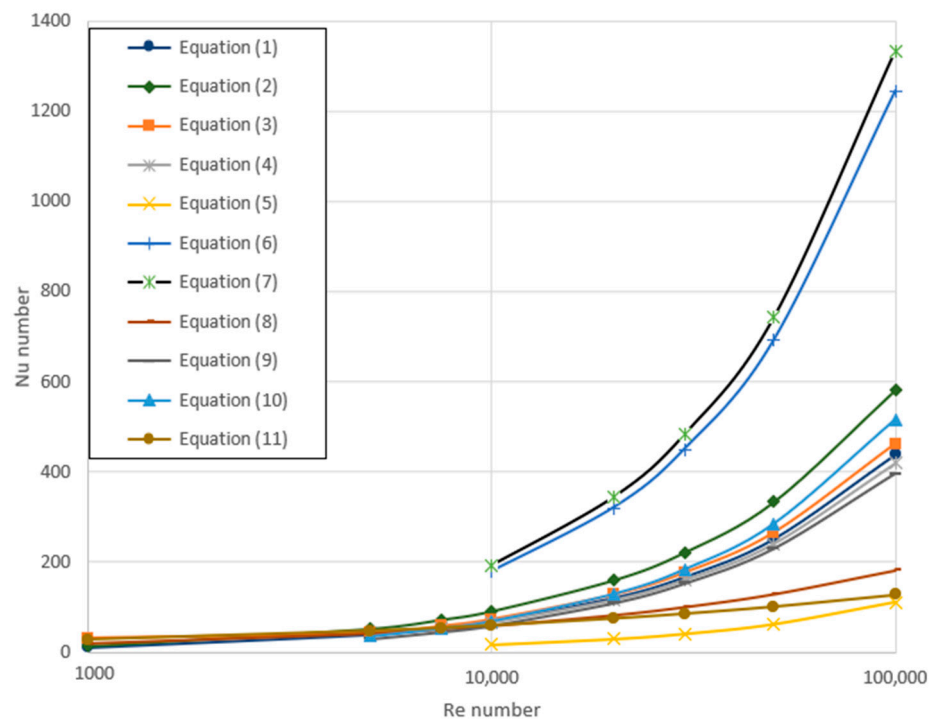


Figure 1. Nu-Re relationships for water.

Table 3. Nu number correlation equations for water- Al₂O₃ nanofluids.

Authors	Equation	Remarks	Equation
Xuan and Li [60]	$\overline{Nu} = 0.0059 \left(1 + 7.6286 \varphi_v^{0.6886} Pe_p^{0.001} \right) Re^{0.9238} Pr^{0.4}$	$Pe_p = \frac{wd_p}{a_{nf}}$	Equation (12)
Vasu et al. [61]	$\overline{Nu} = 0.0256 \cdot Re^{0.8} Pr^{0.4}$	$10^4 < Re < 8 \times 10^4$	Equation (13)
Hussein et al. [62]	$\overline{Nu} = 0.02 \cdot Re^{0.788} Pr^{0.45}$	$5000 < Re < 5 \times 10^4$ $6.8 < Pr < 11.97$	Equation (14)
Sahin et al. [63]	$\overline{Nu} = 0.106 \cdot Re^{0.588} \cdot (1 + \varphi_v^{-0.1096}) \cdot Pr^{0.258}$	$4000 < Re < 20,000$ $5 < Pr < 7$ $0.5\% < \varphi_v < 4\%$	Equation (15)
Chavan and Pise [64]	$\overline{Nu} = 0.508358 \cdot Re^{0.7401} \cdot Pr^{-0.7026}$	$6000 < Re < 14,000$ $0.3\% < \varphi < 1\%$	Equation (16)
Durga and Gupta [65]	$\overline{Nu} = 0.09589 \cdot Re^{0.8} \cdot Pr^{0.4} \cdot (1 + \varphi_v)^{2833}$	$3000 < Re < 30,000$ $5.12 < Pr < 6.54$ $0\% < \varphi_v < 0.03\%$	Equation (17)
Saha and Paul [66]	$\overline{Nu} = 0.0126 Re^{0.85589} Pr^{0.44709} \left(\frac{d_f}{d_p} \right)^{-0.00176}$	$10^4 < Re < 10^5$ $8.45 < Pr < 20.29$ $4\% < \varphi_v < 6\%$ $10 < d_p \text{ [nm]} < 40$	Equation (18)



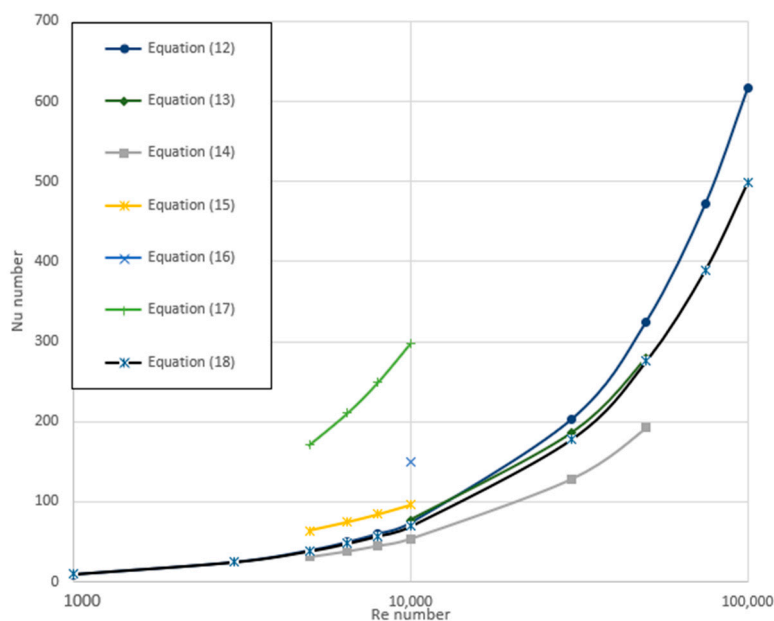


Figure 2. Nu-Re relationships for water-Al₂O₃ nanofluids.

2.3. Correlations for Thermophysical Properties of Nanofluids

A large number of correlations devoted to calculate viscosity of nanofluids are published in the literature, e.g., [67,68]. In Table 4 are shown correlations proposed for water-Al₂O₃ nanofluids.

Table 4. Correlations for viscosity of water- Al₂O₃ nanofluids.

Authors	Correlation	Remarks	Equation
Krieger and Dougherty [69]	$\mu_{nf} = \mu_{bf} \left(1 - \left(\frac{\varphi_a}{\varphi_{vs}} \right)^{-2.5\varphi_m} \right)$	φ_a —volume fraction of aggregates $\varphi_a = \varphi_v (d_a / d_p)^{3-d_f}$ φ_v —volume fraction of the well-dispersed individual particles, d_a —diameter of aggregates, d_f —fractal dimension of aggregates φ_{vs} —volume fraction of densely packed spheres	Equation (19)
Palm et al. [70]	$\mu_{bf} = 0.034 - 2 \cdot 10^{-4} T + 2.9 \cdot 10^{-7} T^2$ $\mu_{bf} = 0.039 - 2.3 \cdot 10^{-4} T + 3.4 \cdot 10^{-7} T^2$	$\varphi_v = 1\%$ $\varphi_v = 4\%$	Equation (20) Equation (21)
Nguyen et al. [71]	$\mu_{nf} = 0.904 e^{0.148\varphi_v} \mu_{bf}$ $\mu_{bf} = (2.1275 - 0.0215 \cdot T + 0.0002 \cdot T^2) \mu_{bf}$	$d_p = 47$ nm $\varphi_v = 4\%$	Equation (22) Equation (23)
Khanafar and Vafai [72]	$\mu_{nf} = -0.4491 + \frac{28.837}{t} + 0.574\varphi_v - 0.1634\varphi_v^2 + 23.053 \frac{\varphi_v^2}{t^2} + 0.0132\varphi_v^3 - 2354.735 \frac{\varphi_v}{t^3} + 23.498 \frac{\varphi_v^2}{d_p^2} - 3.0185 \frac{\varphi_v^3}{d_p^3}$		Equation (24)
Pastoriza-Gallego et al. [73]	$\mu_{nf} = e^{(A + \frac{B}{T - T_o}) \varphi_v}$		Equation (25)
		φ_v	
	A	0.000 0.005 0.010 0.015 0.021 0.031 0.048	
	B [K]	−3.694 −3.632 −2.381 −1.702 −3.450 −3.302 −1.379	
	T _o [K]	999.0 999.0 689.3 534.7 999.0 999.0 518.4	
		145.7 145.5 169.8 185.5 146.2 145.3 189.9	

Table 4. Cont.

Authors	Correlation	Remarks	Equation
Corcione [74]	$\mu_{nf} = \mu_{bf} \left(\frac{1}{1 - 34.87 \left(\frac{d_p}{d_f} \right)^{-0.3} \varphi_v^{1.03}} \right)$	d_f —equivalent diameter of liquid molecule $d_f = 0.1 \left(\frac{6M}{N\pi\rho_{fo}} \right)^{1/3}$ M —molecular weight of water N —Avogadro number ρ_{fo} — density of water at $T_o = 293$ K	Equation (26)

The correlation proposed by Corcione, Equation (26), was selected for the analysis, as it fits the experimental data of the viscosity of water- Al_2O_3 nanofluids very well.

Equally important as reliable correlations for nanofluids are the formulas for calculating the properties of base liquids. Tested correlations for calculation viscosity of water are shown in Table 5.

Table 5. Correlations for viscosity of water.

Authors	Correlation	Range	Equation
Minea et al. Equation (31) in [36]	$\mu_{bf} = 1.055787 - 0.0132897 \cdot T + 0.00006309 \cdot T^2 - 1.337306666 \cdot 10^{-7} \cdot T^3 - 1.06666666 \cdot 10^{-10} \cdot T^4$	$294 < T < 344$	Equation (27)
Chon and Khim [75]	$\mu_{bf} = 2.414 \cdot 10^{-5} \cdot 10^{\frac{247.8}{T-140}}$	$294 < T < 344$	Equation (28)
Purohit et al. [76]	$\mu_{bf} = 999.79 + 0.068 \cdot t - 0.0107 \cdot t^2 + 0.00082 \cdot t^{2.5} - 2.303 \cdot 10^{-5} \cdot t^3$	$300 < T < 350$	Equation (29)
Saeed and Dulaimi [77]	$\mu_{bf} = 0.414092804247831 - 4.792184560427 \cdot 10^{-3} T + 2.0927097596 \cdot 10^{-5} T^2 - 4.0781184 \cdot 10^{-8} T^3 + 2.9885 \cdot 10^{-11} \cdot T^4$		Equation (30)
Present work [78]	$\mu_{bf} = 2.2551419 - 0.033948 \cdot T + 0.0002053 \cdot T^2 - 6.229 \cdot 10^{-7} \cdot T^3 + 9.4741 \cdot 10^{-10} \cdot T^4 - 5.775 \cdot 10^{-13} \cdot T^5$	$283 < T < 343$	Equation (31)

Figure 3 shows the viscosity of water against temperature calculated from correlations presented in Table 5. As seen in Figure 3, predictions realized with Equation (27) deviate by about 20% for minimum temperature 20 °C. Higher temperature difference between predictions is negligible.

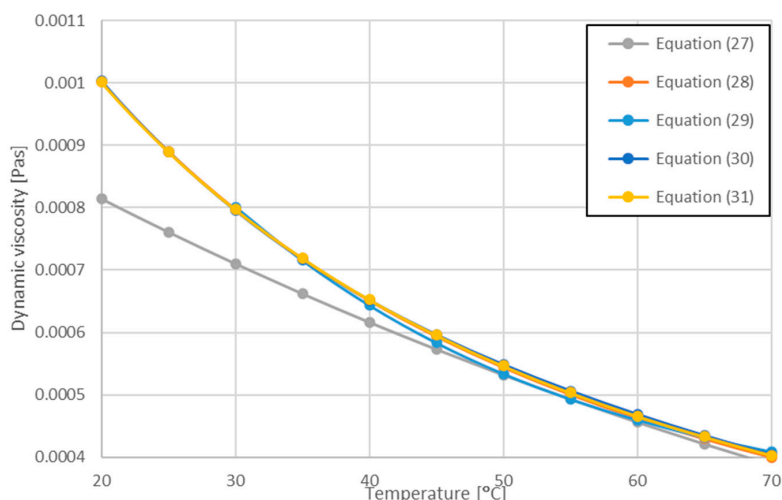


Figure 3. Viscosity of water.

Figure 4 shows influence of NPC on the viscosity of the tested nanofluids against temperature, calculated by the use of Equation (26) in combination with Equation (31).

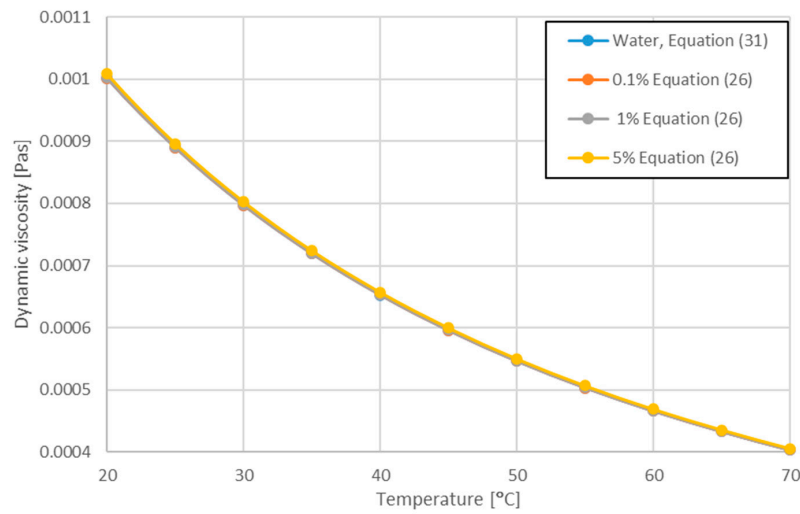


Figure 4. Viscosity of water-Al₂O₃ nanofluids.

As seen in Figure 4, viscosity of the tested nanofluids decreases sharply with a temperature increase and slightly increases with NPC increase. The slight influence of nanoparticles on the viscosity of the tested nanofluids is due to the very small used NPC.

Similarly to viscosity several correlations devoted to thermal conductivity of nanofluids are published in literature, e.g., [79,80]. In Table 6 are collected correlations proposed for water-Al₂O₃ nanofluids.

Table 6. Correlations for thermal conductivity of water- Al₂O₃ nanofluids.

Authors	Correlation	Remarks	Equation
Khanafer and Vafai [72]	$k_{nf} = k_{bf} \left(0.9843 + 0.398 \varphi_v^{0.7383} \left(\frac{1}{d_p} \right)^{0.2246} \left(\frac{\mu_{nf}}{\mu_{bf}} \right)^{0.0235} - 3.9517 \frac{\varphi_v}{t} + 34.034 \frac{\varphi_v^2}{t^3} + 32.509 \frac{\varphi_v}{t^2} \right)$	water-Al ₂ O ₃ 0.01 ≤ φ _v ≤ 0.09 20 ≤ t [°C] ≤ 70 13 nm ≤ d _p ≤ 131 nm	Equation (32)
Corcione [74]	$k_{nf} = k_{bf} \left(1 + 4.4 Re_p^{0.4} Pr^{0.66} \left(\frac{T}{T_{fr}} \right)^{10} \left(\frac{\lambda_p}{\lambda_f} \right)^{0.03} \varphi_v^{0.66} \right)$	Re _p —Re number based on nanoparticle diameter $Re_p = \frac{\rho_{bf} u_B d_p}{\mu_{bf}}$ u _B —Brownian velocity of the nanoparticle $u_B = \frac{2k_b T}{\pi \mu_{bf} d_p^2}$	Equation (33)
Chen [81]	$k_p = k_{nf} \frac{0.75 d_p / l_p}{0.75 d_p / l_p + 1}$	l _p —mean free path of nanoparticle	Equation (34)
Hassani et al. [82]	$k_{nf} = k_{bf} \left(1.04 + \varphi_v^{1.11} \left(\frac{k_p}{k_{bf}} \right)^{0.33} Pr^{-1.7} \left[\frac{1}{Pr^{-1.7}} - \frac{262}{\left(\frac{k_p}{k_{bf}} \right)^{0.33}} + \left(135 \left(\frac{d_{ref}}{d_p} \right)^{0.23} \left(\frac{v_{bf}}{d_p u_{Br}} \right)^{0.82} \right) \left(\frac{c_p}{T^{-1} u_{Br}^2} \right)^{-0.1} \left(\frac{T_B}{T} \right)^{-7} \right] \right)$	Various base fluids, metal and oxide nanoparticles	Equation (35)
Sawicka et al. [83]	$k_{nf} = k_{bf} \left(1 + 0.1046 \varphi_m^{0.2388} \left(\frac{100}{d_p} \right)^{3.14 \cdot 10^{-3}} \right)$		Equation (36)

The correlation proposed by Corcione, Equation (33), was selected for the analysis, as it fits the experimental data of the thermal conductivity of water-Al₂O₃ nanofluids very well, as it takes into account the influence of Brownian motion on the thermal conductivity of nanofluids.

Correlations for calculation thermal conductivity of water are shown in Table 7.

Table 7. Correlations for thermal conductivity of water.

Authors	Correlation	Range	Equation
Minea et al. Equation (22) in [36]	$k_{bf} = -0.98249 \cdot 10^{-5} \cdot T^2 + 7.535211 \cdot 10^{-3} \cdot T - 0.76761$	$294 < T < 344$	Equation (37)
Minea et al. Equation (30) in [36]	$k_{bf} = -0.743567 + 0.077513 \cdot T - 9.9999999 \cdot 10^{-6} \cdot T^2 - 8.63331959 \cdot 10^{-18} \cdot T^3 + 7.301424 \cdot 10^{-21} \cdot T^4$	$294 < T < 344$	Equation (38)
Purohit [76]	$k_{bf} = 0.56112 + (0.00193 \cdot t) - (2.601 \cdot 10^{-6} \cdot t^2) - (6.08 \cdot 10^{-8} \cdot t^3)$	$300 < T < 350$	Equation (39)
Saeed and Dulaimi [77]	$k_{bf} = -0.46662403 + 0.00575419 \cdot T - 7.18 \cdot 10^{-6} \cdot T^2$		Equation (40)
Present work [78]	$k_{bf} = 27.689 - 0.415 \cdot T + 0.000249 \cdot T^2 - 7.389 \cdot 10^{-6} \cdot T^3 + 1.0839 \cdot 10^{-8} - 6.3292 \cdot 10^{-12}$	$283 < T < 343$	Equation (41)

Figure 5 shows thermal conductivity of water against temperature calculated from correlations presented in Table 7.

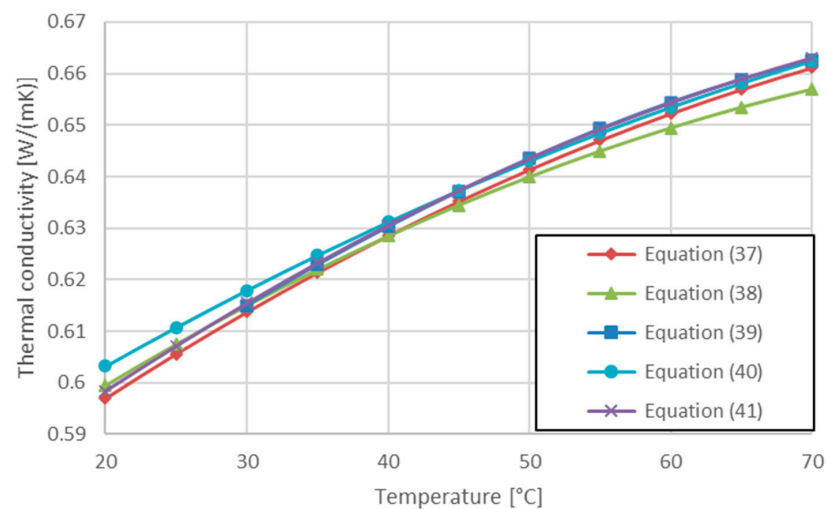


Figure 5. Thermal conductivity of water.

Figure 6 shows influence of NPC on the thermal conductivity of the tested nanofluids against temperature calculated by use of Equation (33) in combination with Equation (41).

As seen in Figure 6 thermal conductivity of the tested nanofluids increases moderately with temperature increase and for given temperature increases with NPC increase.

The density of nanofluids is generally calculated by the use of the mixture model (Table 8).

The correlation proposed by Pak and Cho, Equation (43), was selected for the analysis, as it fits the experimental data of the density of water- Al_2O_3 nanofluids very well and is based on the general mixture theory.

Density of pure water can be estimated by use of correlations given in Table 9.

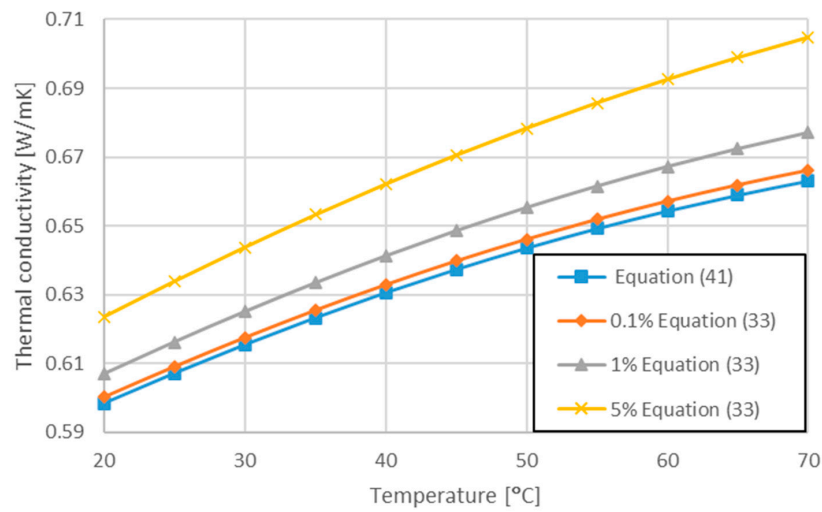


Figure 6. Thermal conductivity of water-Al₂O₃ nanofluids.

Table 8. Correlations for density of nanofluids.

Authors	Correlation	Remarks	Equation
Khanafar and Vafai [72]	$\rho_{nf} = 1001.064 + 2738.6191\varphi_v - 0.2095 \cdot t$	water-Al ₂ O ₃ $0 \leq \varphi_v \leq 0.04$ $5 \leq t[^\circ\text{C}] \leq 40$	Equation (42)
Pak and Cho [84]	$\rho_{nf} = \varphi_v \rho_p + (1 - \varphi_v) \rho_{bf}$	Mixture model	Equation (43)
Sharifpur et al. [85]	$\rho_{nf,nl} = \frac{\rho_{nf}}{(1 - \varphi_v) + \varphi_v (r_p + t_v)^3 / r_p^3}$	r_p —radius of nanoparticle t_v —nanolayer thickness $t_v = -0002833r_p^3 + 0.0475r_p - 0.1417$	Equation (44)

Table 9. Correlations for density of water.

Autors	Correlation	Range	Equation
Minea et al. Equation (20) in [36]	$\rho_{bf} = -2.0546 \cdot 10^{-10} \cdot T^5 + 4.0505 \cdot 10^{-7} \cdot T^4 - 3.1285 \cdot 10^{-4} \cdot T^3 + 0.11576 \cdot T^2 - 20.674 \cdot T + 2446$		Equation (45)
Minea et al. Equation (28) in [36]	$\rho_{bf} = -413.15683 + 13.24245 \cdot T - 0.040578 \cdot T^2 + 0.00004 \cdot T^3 - 2.27018 \cdot 10^{-17} \cdot T^4$		Equation (46)
Purohit et al. [76]	$\rho_{bf} = 999.79 + 0.068 \cdot t - 0.0107 \cdot t^2 + 0.00082 \cdot t^{2.5} - 2.303 \cdot 10^{-5} \cdot t^3$	$300 < T < 350$	Equation (47)
Saeed and Dulaimi [77]	$\rho_{bf} = 765.33 + 1.8142 \cdot T - 0.0035 \cdot 10^{-2} \cdot T^2$		Equation (48)
Present work [78]	$\rho_{bf} = -5859.3637 + 98.96855 \cdot T + 0.574747 \cdot T^2 + 0.0016856 \cdot T^3 - 2.4989 \cdot 10^{-6} \cdot T^4 - 1.4908 \cdot 10^{-9} \cdot T^5$		Equation (49)
Saha and Paul [86]	$\rho_{bf} = 330.12 + 5.92 \cdot T - 1.63 \cdot 10^{-2} \cdot T^2 + 1.33 \cdot 10^{-5} \cdot T^3$	$278 < T < 363$	Equation (50)

Figure 7 shows the density of water against temperature calculated from correlations presented in Table 9. The maximum difference between the predictions is equal to 0.4%.

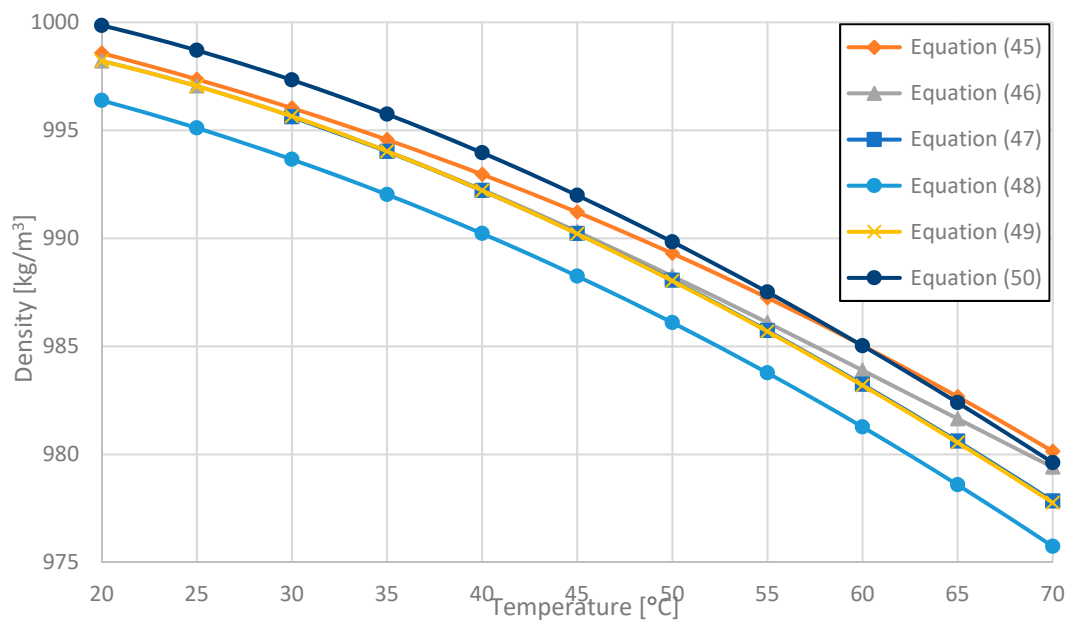


Figure 7. Density of water.

Figure 8 illustrates influence of the NPC on density of the tested nanofluids as a function of temperature by use of Equations (43) and (49).

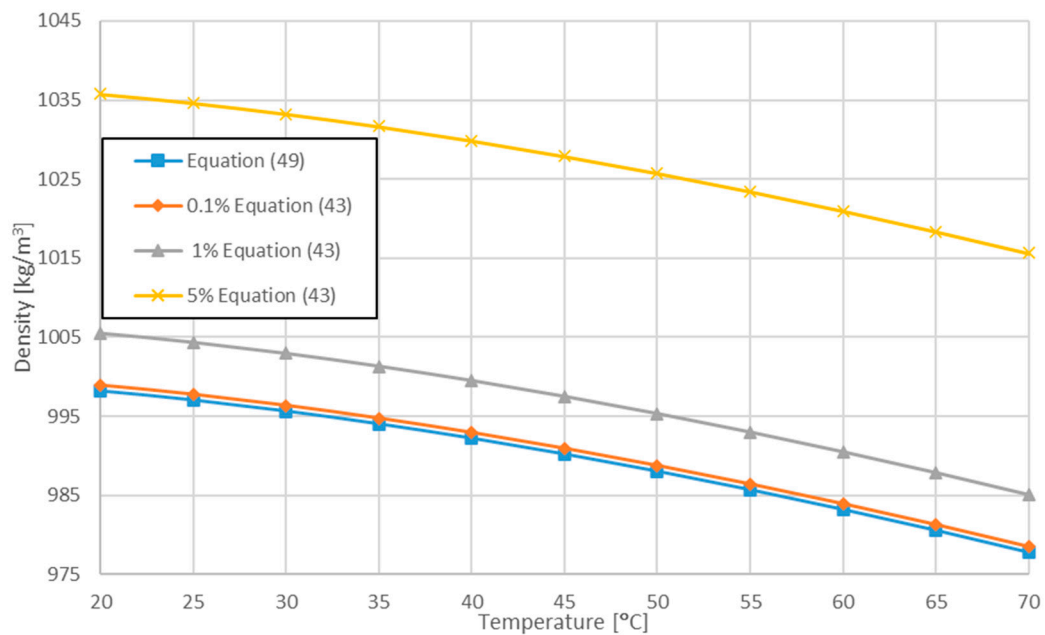


Figure 8. Density of water-Al₂O₃ nanofluids.

As seen in Figure 8, the density of the analysed nanofluids decreases with temperature increase and increases with NPC increase because the density of the nanoparticle material (Table 1) is higher than density of water.

Several investigators have been involved in the physics of the specific heat of nanofluids [87–89]. In Table 10 are collected correlations proposed for water-Al₂O₃ nanofluids.

Table 10. Correlations for specific heat of nanofluids.

Authors	Correlation	Remarks	Equation
Pak and Cho [84]	$c_{p,nf} = \varphi_v c_{p,p} + (1 - \varphi_v) c_{p,bf}$	Mixture model	Equation (51)
Williams et al. [90]	$c_{p,nf} = \frac{\rho_{bf} c_{p,bf} (1 - \varphi_v) + \varphi_v \rho_p c_{p,p}}{\rho_{bf}}$	water-Al ₂ O ₃ , water-ZrO ₂	Equation (52)
Corcione et al. [91]	$c_{p,nf} = \frac{(1 - \varphi_v)(\rho c_p)_{bf} + \varphi_v(\rho c_p)_p}{(1 - \varphi_v)\rho_{bf} + \varphi_v\rho_p}$	water-Al ₂ O ₃ , water-CuO, water-TiO ₂	Equation (53)
Sekhar and Sharma [92]	$c_{p,nf} = c_{p,H_2O} \left[0.8429 \left(1 + \frac{t}{50} \right)^{-0.3037} \left(1 + \frac{d_p}{50} \right)^{0.4167} \left(1 + \frac{\varphi_v}{100} \right)^{2.272} \right]$	water-Al ₂ O ₃ , water-CuO, water-TiO ₂ , water-SiO ₂ 0.01% ≤ φ_v ≤ 4%, 20 ≤ t [°C] ≤ 50, 15 nm ≤ d_p ≤ 50 nm	Equation (54)

The correlation proposed by Williams et al. [90] was selected for the analysis. As shown in [49] Equation (52) much better fits the experimental data of the specific heat of water-Al₂O₃ nanofluids than Equation (51) based on the mixture theory. The better accuracy of Equation (52) results from the assumption of thermal equilibrium between the particles and the liquid, which does not have to be present due to the Brownian motion of nanoparticles and different thermophysical properties of the nanoparticle material and the base liquid.

The specific heat of water can be estimated by use of correlations given in Table 11.

Table 11. Correlations for specific heat of water.

Authors	Correlation	Range	Equation
Minea et al. Equation (21) in [36]	$c_{p,bf} = -2.0546 \cdot 10^{-10} \cdot T^5 + 4.0505 \cdot 10^{-7} \cdot T^4 - 3.1285 \cdot 10^{-4} \cdot T^3 + 0.11576 \cdot T^2 - 20.674 \cdot T + 2446$	293 < T < 313	Equation (55)
Minea et al. Equation (25) in [36]	$c_{p,bf} = 6108.94345 - 12.426 \cdot T + 0.02 \cdot T^2 - 5.540012 \cdot 10^{-12} \cdot T^3 + 6.25929269 \cdot 10^{-21} \cdot T^4$	293 < T < 313	Equation (56)
Saha and Paul [66]	$c_{p,bf} = 10.01 - 5.14 \cdot 10^{-2} \cdot T + 1.49 \cdot 10^{-4} \cdot T^2 - 2.62 \cdot 10^{-12} \cdot T^3$	278 < T < 363	Equation (57)
Purohit et al. [76]	$c_{p,bf} = 4217.4 - 5.61 \cdot T + 1.299 \cdot T^{1.52} - 0.11 \cdot T^2 + 4149.6 \cdot 10^{-6} \cdot T^{2.5}$	300 < T < 350	Equation (58)
Saeed and Dulaimi [77]	$c_{p,bf} = 10444.58656104 - 54.08920728 \cdot T + 0.15359377 \cdot T^2 - 0.00014301 \cdot T^3$		Equation (59)
Present work [78]	$c_{p,bf} = 185614 - 2737 \cdot T + 16.54446 \cdot T^2 - 0.5006 \cdot T^3 + 7.58 \cdot 10^{-5} \cdot T^4 - 4.5942 \cdot 10^{-8} \cdot T^5$	283 < T < 343	Equation (60)

Figure 9 shows the specific heat of water against temperature calculated from correlations presented in Table 11. The difference between the individual correlations seems large, but for 70 °C it does not exceed 3.4%.

As seen in Figure 10, the specific heat of water-Al₂O₃ nanofluids decreases with temperature increases, and for the given temperature decreases with NPC increases because the specific heat of the nanoparticle material (Table 1) is lower than the specific heat of water. It is *worthy to note* the non-monotonic course of specific heat for water-based nanofluids against the temperature that results from the data for water (Figure 9).

Figure 11 illustrates the influence of NPC on thermal diffusivity of the tested nanofluids as a function of temperature. The thermal diffusivity of water was calculated by the use of present correlations, i.e., Equations (41), (49) and (60), while thermal diffusivity of nanofluids was determined by use of Equations (33), (43) and (52). As seen in Figure 11, the thermal diffusivity of water and nanofluids increases with temperature increase, however

the growth rate is higher for nanofluids. Moreover, thermal diffusivity increases with NPC increase.

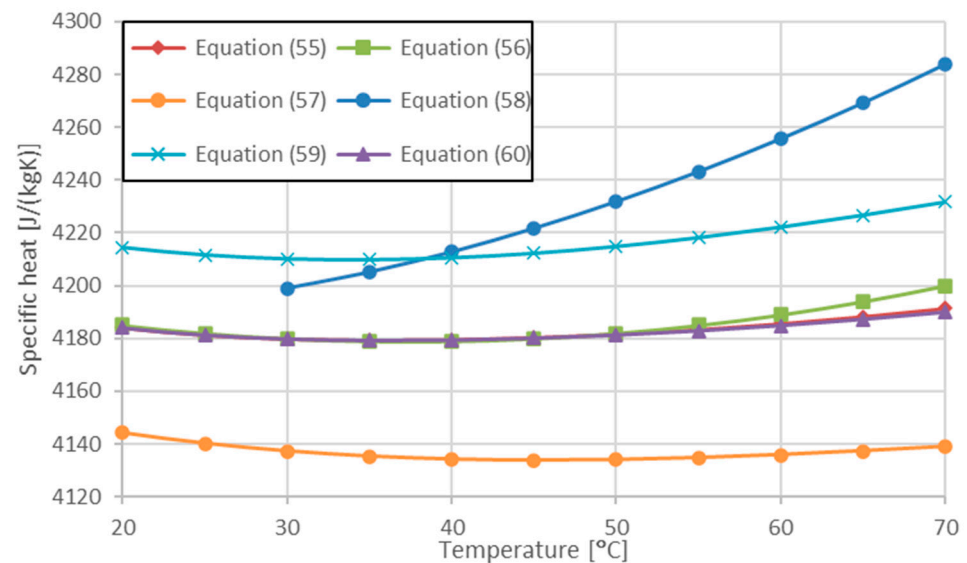


Figure 9. Specific heat of water.

Figure 10 illustrates influence of NPC on the specific heat of the tested nanofluids as a function of temperature calculated by the use of Equation (52) in combination with Equation (60).

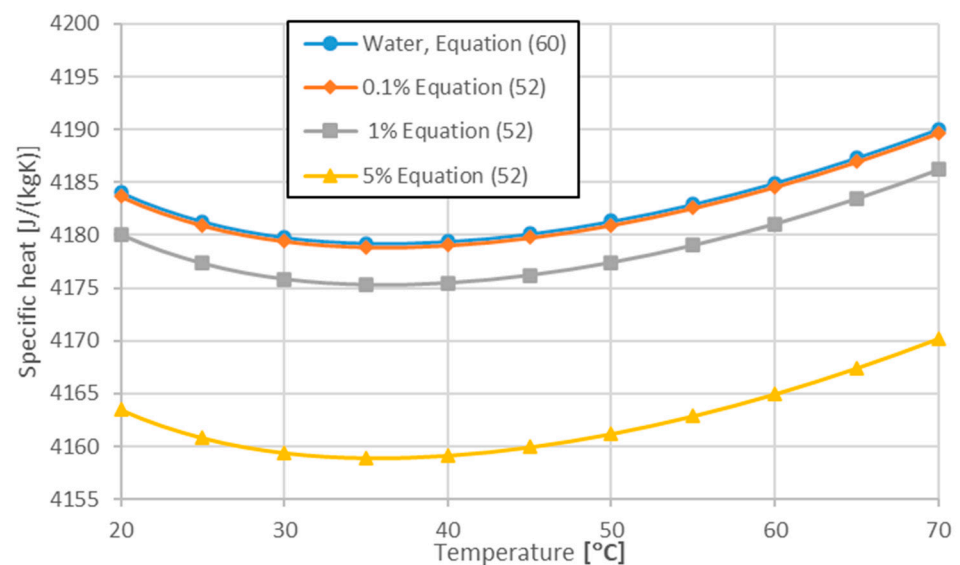


Figure 10. Specific heat of water- Al_2O_3 nanofluids.

As seen in Figure 12, the thermal diffusivity of the tested nanofluids increases slightly with NPC, although the rate of growth increases with temperature increase.

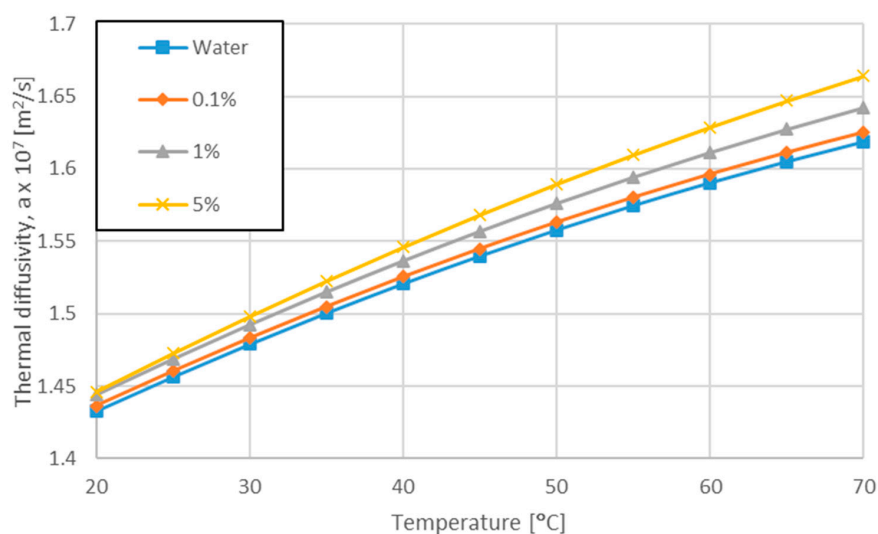


Figure 11. Thermal diffusivity of water-Al₂O₃ nanofluids.

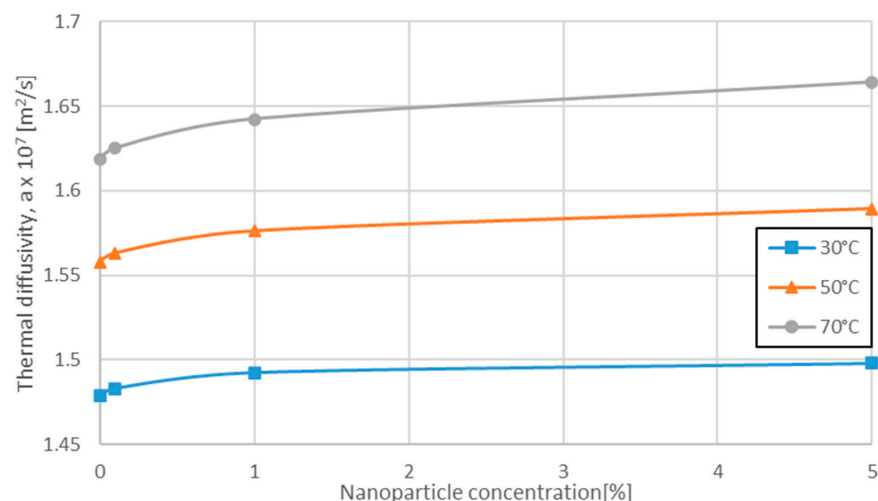


Figure 12. Thermal diffusivity of water-Al₂O₃ nanofluids.

3. Results and Discussion

3.1. Variation of *Pr* Number

Figure 13 shows a comparison of *Pr* numbers of the water-Al₂O₃ nanofluids as a function of temperature. The *Pr* number for water was calculated by use of present correlations, i.e., Equations (31), (41), (49) and (60), while the *Pr* number of nanofluids was determined by use of Equations (26), (33), (43) and (52). For the tested nanofluids, the *Pr* number decreases with an increase in temperature, predominantly due to the decrease in viscosity (Figure 4).

Figure 14 illustrates the influence of NPC on *Pr* number of the tested nanofluids at three temperatures, namely 30 °C, 50 °C, and 70 °C. As seen in Figure 12, the *Pr* number for water-Al₂O₃ decreases slightly with the NPC increase. Regardless of the temperature, the decrease in *Pr* number with the increase in NPC does not exceed 3%.

As shown in Figures 13 and 14, the *Pr* number decreases with both temperature increase and NPC increase. However, the decrease due to the increase in NPC for a given temperature is small, and the decrease due to the increase in temperature is very large for a given NPC. The *Pr* number of the nanofluid for the tested range of temperature and NPC is determined by the temperature, not by the NPC. As it results from the correlations presented in Table 2, the *Nu* number is a function of *Pr*^{*m*}, hence the higher the value of the *Pr* number, the higher the value of the *Nu* number.

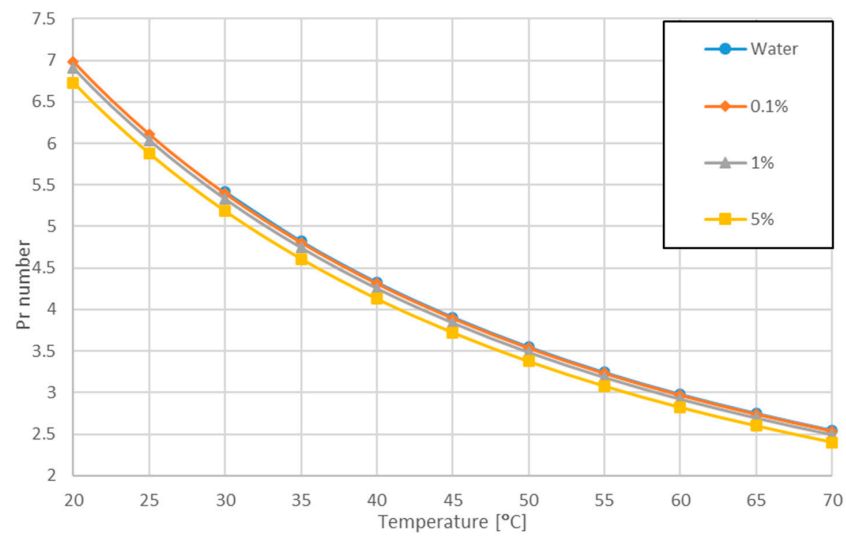


Figure 13. Prandtl number for water- Al_2O_3 nanofluids.

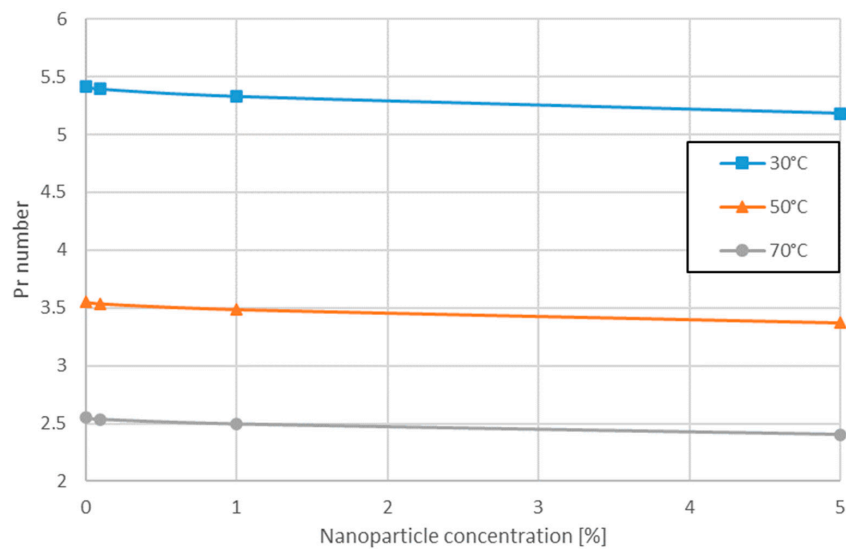


Figure 14. Variation of Pr number for water- Al_2O_3 nanofluids.

3.2. Variation of Re Number

Figure 15 illustrates the change of Re number versus temperature for the tested nanofluids. In this case the average velocity and the diameter of the horizontal tube are held constant at the values taken from the experiment presented in [93], i.e., $w = 1$ m/s, $D = 10$ mm. The Re number for water was calculated by use of present correlations, i.e., Equations (31) and (49), while the Re number of nanofluids was determined by use of Equations (26) and (43).

As seen in Figure 15 Re number definitively increases with temperature increase, which also results in increase of the Nu number.

Figure 16 shows the change of Re number against NPC for selected temperatures. It is observed that an increase in NPC results in a gradual increase of Re number for all tested temperatures.

As shown in Figures 15 and 16, Re number increases with both temperature increase and NPC increase. However, the increase due to the increase in NPC for a given temperature is small, and the increase due to the increase in temperature is substantial. It follows that the value of the Re number in the studied temperature and NPC range is primarily determined by temperature, and the influence of NPC is modest.

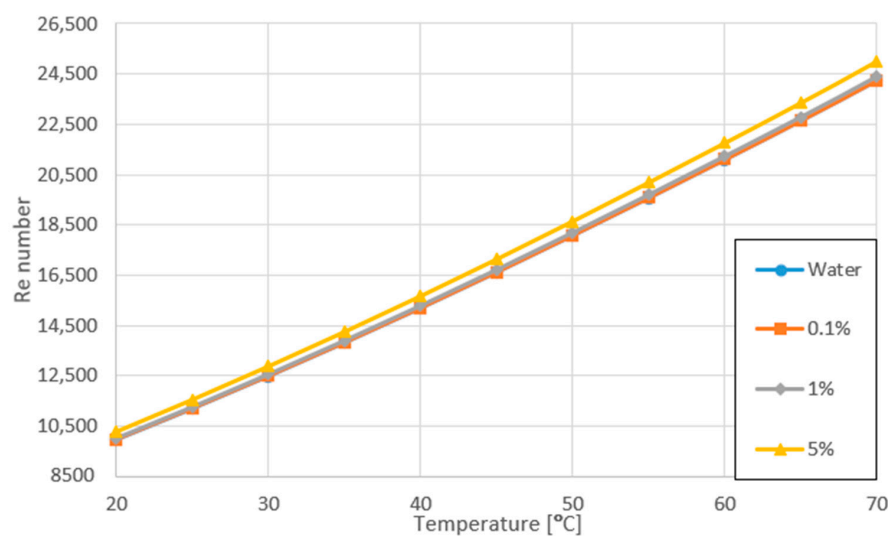


Figure 15. Variation of Re number for water- Al_2O_3 nanofluids.

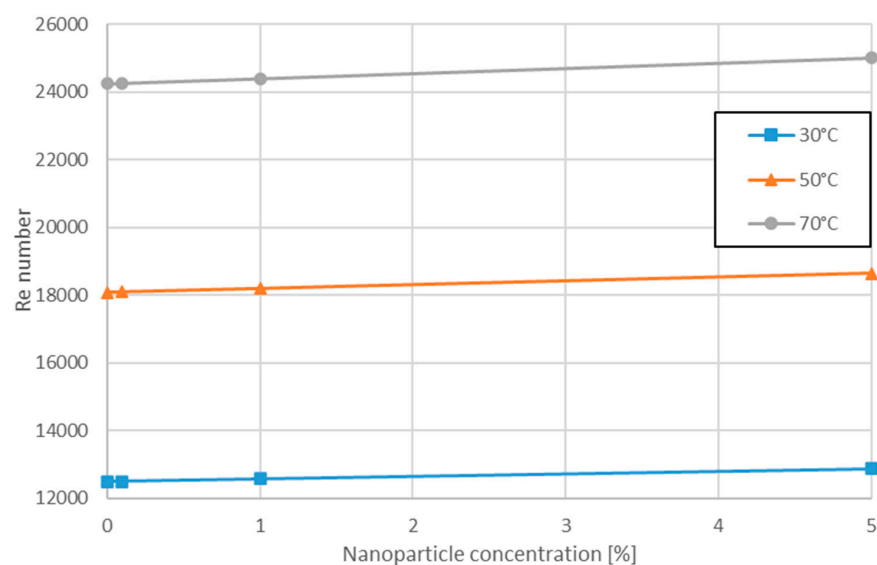


Figure 16. Variation of Re number for water- Al_2O_3 nanofluids.

3.3. Variation of Nu Number

Figure 17 shows the variation of Nu number against temperature for water- Al_2O_3 nanofluids predicted from the Saha and Paul correlation, Equation (18). Results are compared to the predictions for water from the commonly accepted Gnieliński correlation, Equation (10). Calculations for water were conducted by the use of present correlations for thermophysical properties of water. As seen in Figure 17, Nu number increases with temperature increase. For the tested NPC range $0.1\% \leq \varphi_m \leq 5\%$ Nu number for nanofluids is higher than for pure water. It means that the addition of Al_2O_3 nanoparticles to water results in substantial heat transfer improvement.

The influence of nanoparticles on the Nu number is clearer in Figure 18. Figure 18 shows the variation of the Nu number against NPC for water- Al_2O_3 nanofluids and three selected temperatures, namely 30 °C, 50 °C, and 70 °C. As seen in Figure 18, the addition of even the smallest amount of nanoparticles ($\varphi_m = 0.001$) causes a sharp increase in the Nu number. However, the Nu number increase for $\varphi_m > 0.001$ is negligible, and the increase in the Nu number is practically due to the increase in temperature.

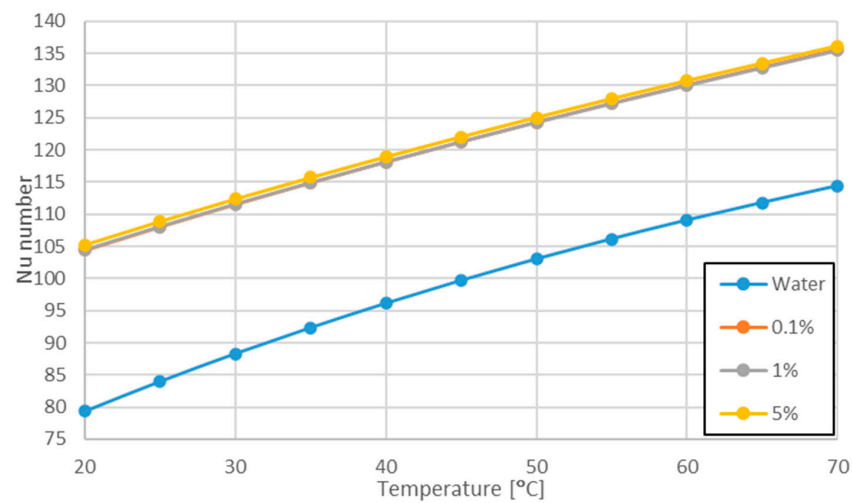


Figure 17. Variation of Nu number for water-Al₂O₃ nanofluids.

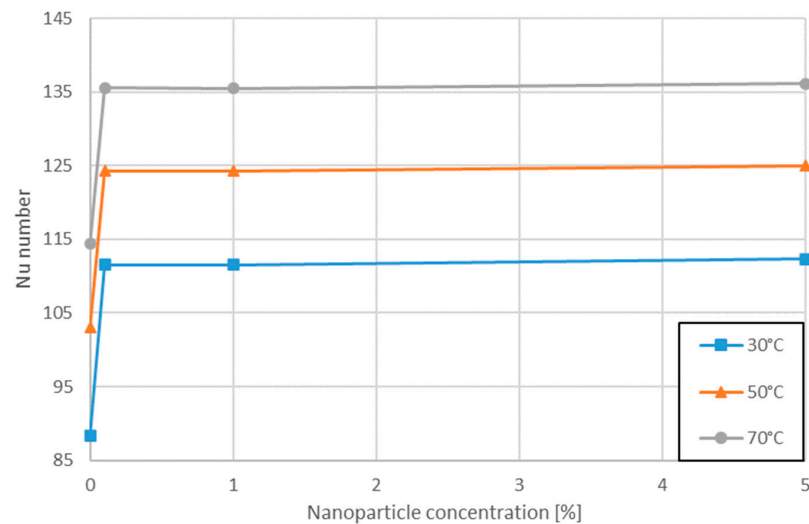


Figure 18. Variation of Nu number for water-Al₂O₃ nanofluids.

3.4. Variation of Heat Transfer Coefficient

Figure 19 shows the variation of heat transfer coefficient against temperature for water-Al₂O₃ nanofluids predicted from the Saha and Paul correlation (Equation (18)). The results are compared to the predictions from the Gnieliński correlation (Equation (10)) for water. As seen in Figure 19, heat transfer coefficient increases with temperature. For the tested mass concentration range $0.1\% \leq \varphi_m \leq 5\%$ heat transfer coefficient for nanofluids is higher than for water. It means that addition of Al₂O₃ nanoparticles to water results in substantial heat transfer improvement. In the literature, several mechanisms of heat transfer improvement in nanofluids have been discussed, e.g., [44,94]. According to Buongiorno [95], two mechanisms are responsible for heat transfer improvement in nanofluids, namely Brownian motion and thermophoresis.

Figure 20 shows variation of heat transfer coefficient against NPC for water-Al₂O₃ nanofluids and three selected temperatures, namely 30 °C, 50 °C and 70 °C. As seen in Figure 20, the influence of NPC on HTC for the tested mass concentration range $0.1\% < \varphi_m \leq 5\%$ is negligible for the given temperature.

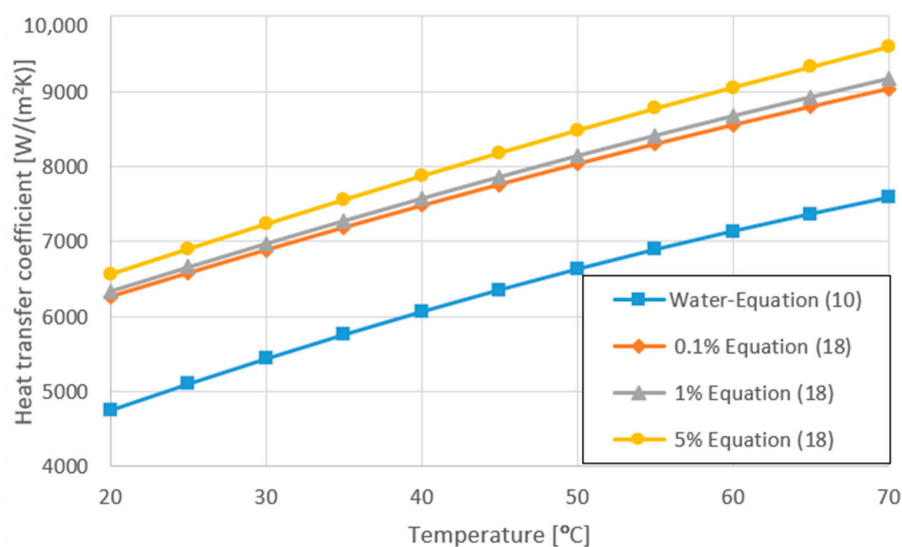


Figure 19. Variation of heat transfer coefficient for water- Al_2O_3 nanofluids.

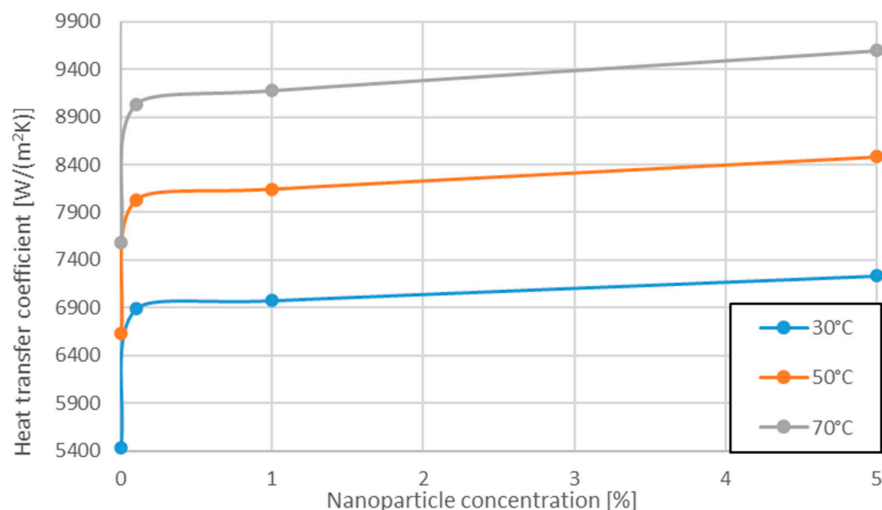


Figure 20. Variation of heat transfer coefficient for water- Al_2O_3 nanofluids.

As shown in Figures 19 and 20, HTC increases with both temperature increase and NPC increase. However, the increase due to the increase in NPC for a given temperature is small, and the increase due to the increase in temperature is significant. It is worth noting that maximum HTC increase is higher than Nu number increase and equals 38%, while for the Nu number it is 31%.

4. Conclusions

The analysis showed that the addition of Al_2O_3 nanoparticles with a mass concentration of $0.1\% \leq \varphi_m \leq 5\%$ within the temperature range of 20–70 °C to water as a base liquid causes the intensification of heat transfer under conditions of turbulent forced convection in round tubes.

The slight influence of the studied concentration of nanoparticles on the thermophysical properties of nanofluids indicates that the intensification of heat transfer results from the transport mechanisms, and not from the improvement of the thermophysical properties of nanofluids.

Author Contributions: Conceptualization, J.T.C.; methodology, J.T.C. and S.S.; software, D.L.; validation, J.T.C.; formal analysis J.T.C. and S.S.; investigation, D.L.; data curation, D.L.; writing—original draft preparation, J.T.C.; writing—review and editing, J.T.C. and S.S.; funding acquisition, S.S. All authors have read and agreed to the published version of the manuscript.

Funding: This research received no external funding.

Institutional Review Board Statement: Not applicable.

Informed Consent Statement: Not applicable.

Data Availability Statement: Not applicable.

Acknowledgments: The authors thank Paweł Dąbrowski (Gdańsk University of Technology) for developing present correlations for thermal properties of water.

Conflicts of Interest: The authors declare no conflict of interest.

Nomenclature

a	Thermal diffusivity	(m ² /s)
c_p	Specific heat	(J/(kgK))
d_f	Base fluid molecule diameter	(m)
d_p	Particle diameter	(m)
D	Inside diameter of tube	(m)
f	Friction factor	(-)
h	Local heat transfer coefficient	(W/(m ² K))
\bar{h}	Average heat transfer coefficient	(W/(m ² K))
k	Thermal conductivity	(W/(m K))
L	Length	(m)
$Nu = \frac{hD}{k}$	Local Nusselt number	(-)
$\bar{Nu} = \frac{\bar{h}D}{k}$	Average Nusselt number	(-)
$Pe = RePr$	Peclet number	(-)
$Pe_p = \frac{wd_p}{a_{nf}}$	Peclet number related to d_p	(-)
$Pr = \frac{\nu}{a}$	Prandtl number	(-)
q	Heat flux	(W/m ²)
$Re = \frac{wD}{\nu}$	Reynolds number	(-)
t	Temperature	[°C]
T	Temperature	[K]
w	Velocity	(m/s)
x	Axial coordinate	(m)

Greek symbols

μ	Dynamic viscosity	(Pas)
ν	Kinematic viscosity	(m ² /s)
ρ	Density	(kg/m ³)
φ	Nanoparticle concentration	(-)

Subscripts

bf	Base fluid
f	Fluid
m	Mass
nf	Nanofluid
nl	Nanolayer
p	Particle
v	Volume
w	Wall

Abbreviations

HTC	Heat transfer coefficient
NPC	Nanoparticle concentration



References

1. Webb, R.L. *Principles of Enhanced Heat Transfer*; John Wiley & Sons, Inc.: New York, NY, USA, 1994.
2. Xie, S.; Beni, M.S.; Cai, J.; Zhao, J. Review of critical-heat-flux enhancement methods. *Int. J. Heat Mass Transf.* **2018**, *122*, 275–289. [\[CrossRef\]](#)
3. Mousa, M.H.; Miljkovic, N.; Nawaz, K. Review of heat transfer enhancement techniques for single phase flows. *Renew. Sustain. Energy Rev.* **2021**, *137*, 110566. [\[CrossRef\]](#)
4. Choi, S. Enhancing thermal conductivity of fluids with nanoparticles. In *Developments and Applications of Non-Newtonian Flows*; ASME: New York, NY, USA, 1995; Volume 231/MD, pp. 99–105.
5. Liang, G.; Mudawar, I. Review of single-phase and two-phase nanofluid heat transfer in macro-channels and micro-channels. *Int. J. Heat Mass Transf.* **2019**, *136*, 324–354. [\[CrossRef\]](#)
6. Lodhi, M.S.; Sheorey, T.; Dutta, G. Single-phase fluid flow and heat transfer characteristics of nanofluid in a circular microchannel: Development of flow and heat transfer correlations. *Proc. Inst. Mech. Eng. C J. Mech. Eng. Sci.* **2020**, *234*, 3689–3708. [\[CrossRef\]](#)
7. Cheng, L.; Filho, E.P.B.; Thome, J.R. Nanofluid Two-Phase Flow and Thermal Physics: A New Research Frontier of Nanotechnology and Its Challenges. *J. Nanosci. Nanotechnol.* **2008**, *8*, 3315–3332. [\[CrossRef\]](#) [\[PubMed\]](#)
8. Dey, D.; Sahu, D.S. Nanofluid in the multiphase flow field and heat transfer: A review. *Heat Transf.* **2021**, *50*, 3722–3775. [\[CrossRef\]](#)
9. Nkurikiyimfura, I.; Wang, Y.; Pan, Z. Heat transfer enhancement by magnetic nanofluids—A review. *Renew. Sustain. Energy Rev.* **2013**, *21*, 548–561. [\[CrossRef\]](#)
10. Shaw, S.; Mabood, F.; Muhammad, T.; Nayak, M.K.; Alghamdi, M. Numerical simulation for entropy optimized nonlinear radiative flow of GO- Al_2O_3 magneto nanomaterials with auto catalysis chemical reaction. *Numer. Methods Partial Differ. Equ.* **2022**, *38*, 329–358.
11. Sivaraj, R.; Banerjee, S. Transport properties of non-Newtonian nanofluids and applications. *Eur. Phys. J. Special Top.* **2021**, *230*, 1167–1171. [\[CrossRef\]](#)
12. Shamshuddin, M.D.; Ghaffari, A.; Usman. Radiative heat energy exploration on Casson-type nanofluid induced by a convectively heated porous plate in conjunction with thermophoresis and Brownian movements. *Int. J. Ambient Energy* **2022**. [\[CrossRef\]](#)
13. Hayat, T.; Aziz, A.; Muhammad, T.; Alsaedi, A. Model and Comparative Study for Flow of Viscoelastic Nanofluids with Cattaneo-Christov Double Diffusion. *PLoS ONE* **2017**, *12*, e0168824. [\[CrossRef\]](#) [\[PubMed\]](#)
14. Li, Y.M.; Al-Khaled, K.; Gouadria, S.; El-Zahar, E.R.; Usman; Khan, S.U.; Khan, M.I.; Malik, M.Y. Numerical simulations for three-dimensional rotating porous disk flow of viscoelastic nanomaterial with activation energy, heat generation and Nield boundary conditions. *Waves Random Complex Media* **2022**. [\[CrossRef\]](#)
15. Mahato, R.; Das, M.; Sen, S.S.S.; Shaw, S. Entropy generation on unsteady stagnation-point Casson nanofluid flow past a stretching sheet in a porous medium under the influence of an inclined magnetic field with homogeneous and heterogeneous reactions. *Heat Transf.* **2022**, *51*, 5723–5747. [\[CrossRef\]](#)
16. Khan, S.U.; Usman; Al-Khaled, K.; Hussain, S.M.; Ghaffari, A.; Khan, M.I.; Ahmed, M.W. Implication of Arrhenius Activation Energy and Temperature-Dependent Viscosity on Non-Newtonian Nanomaterial Bio-Convective Flow with Partial Slip. *Arab. J. Sci. Eng.* **2022**, *47*, 7559–7570. [\[CrossRef\]](#)
17. Zapata, K.; Rodríguez, Y.; Lopera, S.H.; Cortes, F.B.; Franco, C.A. Development of Bio-Nanofluids Based on the Effect of Nanoparticles' Chemical Nature and Novel Solanum torvum Extract for Chemical Enhanced Oil Recovery (CEOR) Processes. *Nanomaterials* **2022**, *12*, 3214. [\[CrossRef\]](#)
18. Mandal, S.; Shit, G.C.; Shaw, S.; Makinde, O.D. Entropy analysis of thermo-solutal stratification of nanofluid flow containing gyrotactic microorganisms over an inclined radiative stretching cylinder. *Therm. Sci. Eng. Prog.* **2022**, *34*, 101379. [\[CrossRef\]](#)
19. Mehta, R.N.; Chakraborty, M.; Parikh, P.A. Nanofuels: Combustion, engine performance and emissions. *Fuel* **2014**, *120*, 91–97. [\[CrossRef\]](#)
20. Cieśliński, J.T.; Krzyżak, J.; Kropiwnicki, J.; Kneba, Z. Experiments on compression ignition engine powered by nano-fuels. *Combust. Engines* **2022**, *188*, 55–59. [\[CrossRef\]](#)
21. Taylor, R.; Coulombe, S.; Otanicar, T.; Phelan, P.; Gunawan, A.; Lv, W.; Rosengarten, G.; Prasher, R.; Tyagi, H. Small particles, big impacts: A review of the diverse applications of nanofluids. *J. Appl. Phys.* **2013**, *113*, 011301. [\[CrossRef\]](#)
22. Humnic, G.; Humnic, A. Application of nanofluids in heat exchangers: A review. *Renew. Sustain. Energy Rev.* **2012**, *16*, 5625–5638. [\[CrossRef\]](#)
23. Sajid, M.U.; Ali, H.M. Recent advances in application of nanofluids in heat transfer devices: A critical review. *Renew. Sustain. Energy Rev.* **2019**, *103*, 556–592. [\[CrossRef\]](#)
24. Mahian, O.; Kolsi, L.; Amani, M.; Estellé, P.; Ahmadi, G.; Kleinstreuer, C.; Marshall, J.S.; Taylor, R.A.; Abu-Nada, E.; Rashidi, S.; et al. Recent advances in modeling and simulation of nanofluid flows-Part II: Applications. *Phys. Rep.* **2019**, *791*, 1–59. [\[CrossRef\]](#)
25. Cieśliński, J.T. *Application of Nanofluids in Thermal Technologies*; Contemporary Issues of Heat and Mass Transfer; Publishing House of the Koszalin University of Technology: Koszalin, Poland, 2019; Tom 1, No. 360; pp. 33–48.
26. Patil, M.; Mehta, D.S.; Guvva, S. Future impact of nanotechnology on medicine and dentistry. *J. Indian Soc. Periodontol.* **2008**, *12*, 34–40.
27. Shaw, S.; Shit, G.C.; Tripathi, D. Impact of drug carrier shape, size, porosity and blood rheology on magnetic nanoparticle-based drug delivery in a microvessel. *Colloids Surf. A Physicochem. Eng. Asp.* **2022**, *639*, 128370. [\[CrossRef\]](#)

28. Kalbande, V.P.; Walke, P.V.; Kriplani, C.V.M. Advancements in Thermal Energy Storage System by Applications of Nanofluid Based Solar Collector: A Review. *Environ. Clim. Technol.* **2020**, *24*, 310–340. [[CrossRef](#)]
29. Li, Z.; Cui, L.; Li, B.; Du, X. Mechanism exploration of the enhancement of thermal energy storage in molten salt nanofluid. *Phys. Chem. Chem. Phys.* **2021**, *23*, 13181. [[CrossRef](#)] [[PubMed](#)]
30. Sundararaj, A.J.; Pillai, B.C.; Asirvatham, L.G. Convective heat transfer analysis of refined kerosene with alumina particles for rocketry application. *J. Mech. Sci. Technol.* **2018**, *32*, 1685–1691. [[CrossRef](#)]
31. Kakaç, S.; Pramuanjaroenki, J.A. Single-phase and two-phase treatments of convective heat transfer enhancement with nanofluids—A state-of-the-art review. *Int. J. Therm. Sci.* **2016**, *100*, 75–97. [[CrossRef](#)]
32. Mahian, O.; Kolsi, L.; Amani, M.; Estellé, P.; Ahmadi, G.; Kleinstreuer, C.; Marshall, J.S.; Siavashi, M.; Taylor, R.A.; Niazmad, H.; et al. Recent advances in modeling and simulation of nanofluid flows—Part I: Fundamentals and theory. *Phys. Rep.* **2019**, *790*, 1–48. [[CrossRef](#)]
33. Solangi, K.H.; Sharif, S.; Sadiq, I.O.; Hisam, M.J. Experimental and numerical investigations on heat transfer and friction loss of functionalized GNP nanofluids. *Int. J. Mech. Eng. Technol.* **2019**, *10*, 61–77.
34. Singh, P.; Oberoi, A.S.; Nijhawan, P. Experimental heat transfer analysis of copper oxide nanofluids through a straight tube. *IJATCSE* **2019**, *8*, 495–500. [[CrossRef](#)]
35. Karabulut, K.; Buyruk, E.; Kilinc, F. Experimental and numerical investigation of convection heat transfer in a circular copper tube using graphene oxide nanofluid. *J. Braz. Soc. Mech. Sci.* **2020**, *42*, 230. [[CrossRef](#)]
36. Kong, M.; Lee, S. Performance evaluation of Al₂O₃ nanofluid as an enhanced heat transfer fluid. *Adv. Mech. Eng.* **2020**, *12*, 1–13. [[CrossRef](#)]
37. Boertz, H.; Baars, A.J.; Cieśliński, J.T.; Smolen, S. Numerical Study of Turbulent Flow and Heat Transfer of Nanofluids in Pipes. *Heat Transf. Eng.* **2018**, *39*, 241–251. [[CrossRef](#)]
38. Minea, A.A.; Buonomo, B.; Burggraf, J.; Ercole, D.; Karpaiya, K.R.; Pasqua, A.D.; Sekrani, G.; Steffens, J.; Tibaut, J.; Wichmann, N.; et al. NanoRound: A benchmark study on the numerical approach in nanofluids' simulation. *Int. Commun. Heat Mass Transf.* **2019**, *108*, 104292. [[CrossRef](#)]
39. Onyiriuka, E.J.; Ikponmwoba, E.A. A numerical investigation of mango leaves-water nanofluid under laminar flow regime. *Niger. J. Technol.* **2019**, *38*, 348–354. [[CrossRef](#)]
40. Jamali, M.; Toghraie, D. Investigation of heat transfer characteristics in the developing and the developed flow of nanofluid inside a tube with different entrances in the transition regime. *J. Therm. Anal. Calorim.* **2020**, *139*, 685–699. [[CrossRef](#)]
41. Fadodun, O.G.; Amosun, A.A.; Salau, A.O.; Olaloye, D.O.; Ogundegi, J.A.; Ibitoye, F.I.; Balogun, F.A. Numerical investigation and sensitivity analysis of turbulent heat transfer and pressure drop of Al₂O₃/H₂O nanofluid in straight pipe using response surface methodology. *Arch. Thermodyn.* **2020**, *41*, 3–30.
42. Uribe, S.; Zouli, N.; Cordero, M.E.; Al-Dahhan, M. Development and validation of a mathematical model to predict the thermal behaviour of nanofluids. *Heat Mass Transf.* **2021**, *57*, 93–110. [[CrossRef](#)]
43. Angayarkanni, S.A.; Philip, J. Review on thermal properties of nanofluids: Recent developments. *Adv. Colloid Interface Sci.* **2015**, *225*, 146–176. [[CrossRef](#)]
44. Ilyas, S.U.; Pendyala, R.; Marneni, N. Stability of Nanofluids. Topics in Mining, Metallurgy and Materials Engineering. In *Engineering Applications of Nanotechnology. From Energy to Drug Delivery*; Korada, V.S., Hamid, N.H.B., Eds.; Springer: Berlin/Heidelberg, Germany, 2017.
45. Akbari, M.; Galanis, N.; Behzadmehr, A. Comparative assessment of single and two-phase models for numerical studies of nanofluid turbulent forced convection. *Int. J. Heat Fluid Flow* **2012**, *37*, 136–146. [[CrossRef](#)]
46. Moraveji, M.K.; Esmaeili, E. Comparison between Single-Phase and Two-Phases CFD Modeling of Laminar Forced Convection Flow of Nanofluids in Circular Tube under Constant Heat Flux. *Int. Commun. Heat Mass Transf.* **2012**, *39*, 1297–1302. [[CrossRef](#)]
47. Duan, F. *Thermal Property Measurement of Al₂O₃-Water Nanofluids*. *Smart Nanoparticles Technology*; Abbass, H., Ed.; InTech: London, UK, 2012; ISBN 978-953-51-0500-8.
48. Buongiorno, J.; Venerus, D.C.; Prabhat, N.; McKrell, T.; Townsend, J.; Christianson, R.; Tolmachev, Y.V.; Keblinski, P.; Hu, L.-w.; Alvarado, J.L.; et al. A benchmark study on the thermal conductivity of nanofluids. *J. Appl. Phys.* **2009**, *106*, 094312. [[CrossRef](#)]
49. Vajjha, R.S.; Das, D.K. Specific heat measurement of three nanofluids and development of new correlations. *ASME J. Heat Transf.* **2009**, *131*, 071601–071607. [[CrossRef](#)]
50. Dittus, F.W.; Boelter, L.M.K. Heat transfer in automobile radiators of the tubular type. *Univ. Calif. Publ. Eng.* **1930**, *2*, 443–461. [[CrossRef](#)]
51. Kraußold, H. *Die Wärmeübertragung an Flüssigkeiten in Röhren bei turbulenter Strömung*. *Forschung auf dem Gebiet des Ingenieurwesens*; Springer: Berlin/Heidelberg, Germany, 1933; Band 1; pp. 39–44.
52. Sieder, E.N.; Tate, G.E. Heat transfer and pressure drop of liquids in tubes. *Ind. Eng. Chem. Res.* **1936**, *28*, 1429–1435. [[CrossRef](#)]
53. Mikhejev, M.A.; Mikhejeva, I.M. *Teplootdacha pri Turbulentom Dvizhenji w Trubach*; Osnovy teploperedchi, Energija: Moscow, Russia, 1973. (In Russian)
54. Petukhov, B.S. Heat Transfer and Friction in Turbulent Pipe Flow with Variable Physical Properties. *Adv. Heat Transf.* **1970**, *503–564*.
55. Notter, R.H.; Sleicher, C.A. A solution to the turbulent Graetz problem—III fully developed and entry region heat transfer rates. *Chem. Eng. Sci.* **1972**, *27*, 2073–2093. [[CrossRef](#)]

56. Churchill, S.W.; Ozoe, H. Correlations for laminar forced convection in flow over a flat plate and in developing and fully developed flow in a tube. *J. Heat Trans-T ASME* **1973**, *95*, 78–84. [[CrossRef](#)]
57. Hausen, H. Erweiterte Gleichung für den Wärmeübergang in Rohren bei turbulenter Strömung. *Wärme Stoffübertragung* **1974**, *7*, 222–225. [[CrossRef](#)]
58. Gniewiński, V. Neue Gleichungen für den Wärme—und den Stoffübergang in turbulent durchströmten Rohren und Kanälen. In *Forschung in Ingenieurwesen*; Springer: Berlin/Heidelberg, Germany, 1975; Band 41; pp. 8–16.
59. Kutateladze, S.S. *Osnovy teorii Teploobmena*; Atomizdat: Moscow, Russia, 1979. (In Russian)
60. Xuan, Y.; Li, Q. Investigation on Convective Heat Transfer and Flow Features of Nanofluids. *J. Heat Trans-T ASME*. **2003**, *125*, 151–155. [[CrossRef](#)]
61. Vasu, V.; Krishna, K.R.; Kumar, A.C.S. Analytical prediction of forced convective heat transfer of fluids embedded with nanostructured materials (nanofluids). *PRAMANA J. Phys.* **2007**, *69*, 411–421. [[CrossRef](#)]
62. Hussein, A.M.; Sharma, K.V.; Bakar, R.A.; Kadrigama, K. The Effect of Nanofluid Volume Concentration on Heat Transfer and Friction Factor inside a Horizontal Tube. *J. Nanomater.* **2013**, *2013*, 1–12. [[CrossRef](#)]
63. Sahin, B.; Gültekin, G.G.; Manay, E.; Karagoz, S. Experimental investigation of heat transfer and pressure drop characteristics of Al₂O₃-water nanofluid. *Exp. Therm. Fluid Sci.* **2013**, *50*, 21–28. [[CrossRef](#)]
64. Chavan, D.; Pise, A.T. Experimental investigation of convective heat transfer augmentation using Al₂O₃/water nanofluid in circular pipe. *Heat Mass Transf.* **2015**, *51*, 1237–1246. [[CrossRef](#)]
65. Durga Prasad, P.V.; Gupta, A. Experimental investigation on enhancement of heat transfer using Al₂O₃/water nanofluid in a u-tube with twisted tape inserts. *Int. Commun. Heat Mass Transf.* **2016**, *75*, 154–161. [[CrossRef](#)]
66. Saha, G.; Paul, M.C. Heat transfer and entropy generation of turbulent forced convection flow of nanofluids in a heated pipe. *Int. Commun. Heat Mass Transf.* **2015**, *61*, 26–36. [[CrossRef](#)]
67. Meyer, J.P.; Adio, S.A.; Sharifpur, M.; Nwosu, P.N. The Viscosity of Nanofluids: A Review of the Theoretical, Empirical, and Numerical Models. *Heat Transf. Eng.* **2016**, *37*, 387–421. [[CrossRef](#)]
68. Bashirnezhad, K.; Bazri, S.; Safaei, M.R.; Goodarzi, M.; Dahari, M.; Mahian, O.; Dalkılıç, A.S.; Wongwises, S. Viscosity of nanofluids: A review of recent experimental studies. *Int. Commun. Heat Mass Transf.* **2016**, *73*, 114–123. [[CrossRef](#)]
69. Krieger, I.M.; Dougherty, T.J. A mechanism for non-newtonian flow in suspensions of rigid spheres. *Trans. Soc. Rheology.* **1959**, *3*, 137–152. [[CrossRef](#)]
70. Palm, S.J.; Roy, G.; Nguyen, C.T. Heat transfer enhancement with the use of nanofluids in radial flow cooling systems considering temperature dependent properties. *Appl. Therm. Eng.* **2006**, *26*, 2209–2218. [[CrossRef](#)]
71. Nguyen, C.T.; Desgranges, F.; Roy, G.; Galanis, N.; Mare, T.; Boucher, S.; Mintsa, A. Temperature and particle-size dependent viscosity data for water-based nanofluids—Hysteresis phenomenon. *Int. J. Heat Fluid Flow* **2007**, *28*, 1492–1506. [[CrossRef](#)]
72. Khanafer, K.; Vafai, K. A critical synthesis of thermophysical characteristics of nanofluids. *Int. J. Heat Mass Transf.* **2011**, *54*, 4410–4428. [[CrossRef](#)]
73. Pastoriza-Gallego, M.J.; Lugo, L.; Legido, J.L.; Piñeiro, M.M. Thermal conductivity and viscosity measurements of ethylene glycol-based Al₂O₃ nanofluids. *Nanoscale Res. Lett.* **2011**, *6*, 221. [[CrossRef](#)]
74. Corcione, M. Empirical correlating equations for predicting the effective thermal conductivity and dynamic viscosity of nanofluids. *Energy Convers. Manag.* **2011**, *52*, 789–793.
75. Chon, C.H.; Kihm, K.D. Empirical correlation finding the role of temperature and particle size for nanofluid (Al₂O₃) thermal conductivity enhancement. *Appl. Phys. Lett.* **2005**, *87*, 153107. [[CrossRef](#)]
76. Purohit, N.; Purohit, V.A.; Purohit, K. Assessment of nanofluids for laminar convective heat transfer: A numerical study. *Eng. Sci. Technol. Int. J.* **2016**, *19*, 574–586. [[CrossRef](#)]
77. Saeed, F.R.; Al-Dulaimi, M.A. Numerical investigation for convective heat transfer of nanofluid laminar flow inside a circular pipe by applying various models. *Arch. Thermodyn.* **2021**, *42*, 71–95.
78. Lemmon, E.W.; Huber, M.L.; McLinden, M.O. *NIST Standard Reference Database 23, Reference Fluid Thermodynamic and Transport Properties (REFPROP), Version 9.0*; National Institute of Standards and Technology: Gaithersburg, MD, USA, 2010.
79. Kleinstreuer, C.; Feng, Y. Experimental and theoretical studies of nanofluid thermal conductivity enhancement: A review. *Nanoscale Res. Lett.* **2011**, *6*, 229. [[CrossRef](#)]
80. Aybar, H.Ş.; Sharifpur, M.; Azizian, M.R.; Mehrabi, M.; Meyer, J.P. A Review of Thermal Conductivity Models for Nanofluids. *Heat Transf. Eng.* **2015**, *36*, 1085–1110. [[CrossRef](#)]
81. Chen, G. Nonlocal and nonequilibrium heat conduction in the vicinity of nanoparticles. *J. Heat Trans-T ASME* **1996**, *118*, 539–545. [[CrossRef](#)]
82. Hassani, S.; Saidur, R.; Mekhilef, S.; Hepbasli, A. A new correlation for predicting the thermal conductivity of nanofluids; using dimensional analysis. *Int. J. Heat Mass Transfer.* **2015**, *90*, 121–130. [[CrossRef](#)]
83. Sawicka, D.; Ciesliński, J.T.; Smolen, S.A. Comparison of Empirical Correlations of Viscosity and Thermal Conductivity of Water-Ethylene Glycol-Al₂O₃ Nanofluids. *Nanomaterials* **2020**, *10*, 1487. [[CrossRef](#)] [[PubMed](#)]
84. Pak, B.C.; Cho, Y.I. Hydrodynamic and heat transfer study of dispersed fluids with submicron metallic oxide particles. *Exp. Heat Transf.* **1998**, *11*, 151–170. [[CrossRef](#)]
85. Sharifpur, M.; Yousefi, S.; Meyer, J.P. A new model for density of nanofluids including nanolayer. *Int. Commun. Heat Mass Transf.* **2016**, *78*, 168–174. [[CrossRef](#)]

86. Saha, G.; Paul, M.C. Numerical analysis of the heat transfer behaviour of water based Al_2O_3 and TiO_2 nanofluids in a circular pipe under the turbulent flow condition. *Int. Commun. Heat Mass Transf.* **2014**, *56*, 96–108. [[CrossRef](#)]
87. Shahrul, I.M.; Mahbubul, I.M.; Khaleduzzaman, S.S.; Saidur, R.; Sabri, M.F.M. A comparative review on the specific heat of nanofluids for energy perspective. *Renew. Sustain. Energy Rev.* **2014**, *38*, 88–98. [[CrossRef](#)]
88. Riaz, H.; Murphy, T.; Webber, G.B.; Atkin, R.; Tehrani, S.S.M.; Taylor, R.A. Specific heat control of nanofluids: A critical review. *Int. J. Therm. Sci.* **2016**, *107*, 25–38. [[CrossRef](#)]
89. Hentschke, R. On the specific heat capacity enhancement in nanofluids. *Nanoscale Res. Lett.* **2016**, *11*, 88. [[CrossRef](#)]
90. Williams, W.; Buongiorno, J.; Hu, L.W. Experimental investigation of turbulent convective heat transfer and pressure loss of alumina/water and zirconia/water nanoparticle colloids (nanofluids) in horizontal tubes. *J. Heat Trans-T ASME* **2008**, *130*, 042412. [[CrossRef](#)]
91. Corcione, M.; Cianfrini, M.; Quintino, A. Heat transfer of nanofluids in turbulent pipe flow. *Int. J. Therm. Sci.* **2012**, *56*, 58–69. [[CrossRef](#)]
92. Sekhar, Y.R.; Sharma, K.V. Study of viscosity and specific heat capacity characteristics of water-based Al_2O_3 nanofluids at low particle concentrations. *J. Exp. Nanosci.* **2012**, *56*, 58–69.
93. Cieśliński, J.T.; Kozak, P. Experimental investigation of forced convection of water- Al_2O_3 nanofluids inside horizontal tubes. In Proceedings of the XVI International Symposium Heat Transfer and Renewable Sources of Energy, Szczecin-Międzyzdroje, Poland, 10–13 September 2016.
94. Godson, L.; Raja, B.; Lal, D.M.; Wongwises, S. Enhancement of heat transfer using nanofluids—An overview. *Renew. Sustain. Energy Rev.* **2010**, *14*, 629–641. [[CrossRef](#)]
95. Buongiorno, J. Convective Transport in Nanofluids. *J. Heat Transfer* **2006**, *128*, 240–250. [[CrossRef](#)]